ISIJ International, Vol. 55 (2015), No. 9, pp. 1980–1986

An Improved Model for Camber Generation during Rough Rolling Process

Youngil KANG,[1)] Yujin JANG,[2)] Yongjun CHOI,[3)] Dukman LEE[3)] and Sangchul WON[4)]*

1) Control and Automation Laboratory, Graduate Institute of Ferrous Technology, Pohang University of Science and Technology, 77 Cheongam-Ro, Pohang, 790-784 Korea. 2) Department of Information Communication Engineering, Dongguk University, 123, Dongdae-ro, Gyeongju, 780-714 Korea. 3) Technical Research Laboratories, POSCO, 6261, Donghaean-ro, Pohang, 790-300 Korea. 4) Department of Electronic & Electrical Engineering, Pohang University of Science and Technology, 77 Cheongam-Ro, Pohang, 790-784 Korea.

(*Received on February 11, 2015; accepted on May 12, 2015*)

A model to describe the curvature of the centerline of a strip at the delivery side during hot rolling can be used to predict the longitudinal shape of the strip after rolling, and can be useful when designing a controller to reduce camber generation. However, the existing model was obtained from studies about side-slipping, and is based on incorrect assumptions. This paper uses the definition of curvature and tangential angle to clarify why the assumptions of the former model are incorrect. Also, this paper proposes a new model for curvature of the centerline at the delivery side; this model is based on the assumption that the curved strip is generated only by the difference between the velocities of the sides of the strip. The accuracy of the proposed model is validated by FEM simulation.

KEY WORDS: camber; side-slipping; finite element method (FEM).

1. Introduction

Hot rolling mill accepts a slab produced by continuous casting process, then converts it to strip that has predefined thickness. The main concern of the hot rolling process is to maximize productivity, by minimizing the production of poor final product and by stabilizing the process. However, problems due to irregular longitudinal shape of the strip such as the lateral movement of the strip (side-slipping), and the longitudinal bending (camber) are the main factors that cause defects such as strip-edge folds, scrapes and telescoped coils. Also, a curved strip is dangerous because it could strike and damage the side of the process line; such events can cause production stoppages.

Both camber and side-slipping are caused by asymmetric factors during rolling such as thickness deviation, temperature difference, roll gap difference, mill constant variation, and work roll wear of the strip along its transverse direction. Moreover, camber and lateral motion are coupled to each other. When camber generated in the roughing mill remains until the strip is fed into the finishing mill, side-slipping increases during passage through the finishing mill. Therefore, camber should be regulated from an early stage of roughing mill.

A mathematical model that describes generation of camber should calculate the curvature of the centerline of the strip at the delivery side because shape of the curve can be reconstructed if the curvatures of all points and initial tangent vector are known.[1,2)] To produce straight strip after rolling, curvatures should be zero at all points on the centerline.[3)] Therefore, an accurate model of curvature of the centerline of the strip at the delivery side is necessary.

The first study model of the curvature of the centerline at the delivery side was produced by Nakajima *et al.*[4)] In this work, the time varying locations of arbitrary points on the centerline were considered to obtain dynamic relation between side-slipping and wedge ratio. They also derived a model for delivery-side curvature, which is affected by the entry-side curvature and wedge ratio. Shiraishi *et al.*[5)] introduced a modified delivery-side curvature model that includes a camber change coefficient that should be tuned to account for various rolling conditions such as front and back tension.

These two models were obtained by considering two fundamental principles: (1) the curvature at the delivery side of the strip is affected by entry-side curvature scaled by the square of the reduction ratio; (2) the velocity difference between Drive-Side (DS) and Work-Side (WS) at the delivery-side is proportional to the wedge ratio. From these two principles, the delivery-side curvature models were represented using an equation that includes entry-side curvature and wedge ratio.

However, the process used to obtain the delivery-side curvature model contains an inconsistency. Previous researchers assumed that the curvature at the delivery-side is affected by both delivery-side velocity difference and entry-side curvature, but, they also assumed that entry-side curvature is affected only by the entry-side velocity difference; *i.e.*, the cause of the curvature at the entry side differs

* Corresponding author: E-mail: won@postech.ac.kr
DOI: http://dx.doi.org/10.2355/isijinternational.ISIJINT-2015-088

from the cause at the delivery side. To achieve consistency, an assumption that the curved shape of the strip is caused by the velocity difference between DS and WS is needed. In addition, delivery-side velocity difference should be affected by entry-side curvature.

In this paper, a new model for curvature of the centerline of the strip at the delivery side is proposed. The delivery-side velocity difference is represented as an equation that uses the mass-flow principle to include entry-side velocity difference and wedge ratio. The relation between curvature of the strip and velocity difference was found using the definitions of curvature, tangential angle, and tangent vector. Delivery-side curvature of the centerline is represented as an equation that includes entry-side curvature and wedge ratio. A three dimensional FEM simulator for rough rolling process was used to verify the accuracy of the proposed model.

The rest of this paper is organized as follows. The process that obtained the old delivery-side curvature model is reviewed in Section 2. A new model based on the new assumption is proposed in Section 3. Brief explanation for FEM simulator and simulation results are given in Section 4. Finally, a conclusion is represented in Section 5.

2. The Former Mechanical Model for Curvature at the Delivery Side

Shiraishi *et al.*[5] introduced delivery-side curvature model that includes entry-side curvature and wedge ratio as

$$\frac{1}{\rho_2}=\frac{\Delta v_2}{bv_2}+\frac{1}{\lambda^2}\frac{\Delta v_1}{bv_1}=\frac{1}{\lambda^2}\frac{1}{\rho_1}+\frac{\xi}{b}\left(\frac{\Delta h}{h}-\frac{\Delta H}{H}\right). \quad \text{..... (1)}$$

where $1/\rho_2$ is delivery-side curvature, λ is reduction ratio h/H, $1/\rho_1$ is entry-side curvature, b is width of the strip, h is delivery-side strip thickness, H is entry-side strip thickness, ξ is a camber-change coefficient and Δh and ΔH are delivery-side and entry-side wedge respectively. To obtain the model, two assumptions were used: (1) that entry-side velocity difference Δv_1 influences delivery-side curvature $1/\rho_2$ scaled by $1/\lambda^2$ in addition to the curvature due to delivery-side velocity difference Δv_2; and (2) that Δv_2 is proportional to the wedge ratio $\Delta\psi$:

$$\frac{\Delta v_2}{v_2}=\alpha\left[\frac{\Delta h}{h}-\frac{\Delta H}{H}\right]. \quad \text{..... (2)}$$

According to this model, $1/\rho_1$ is only determined by Δv_1, whereas $1/\rho_2$ is affected by both the Δv_2 and $1/\rho_1$.

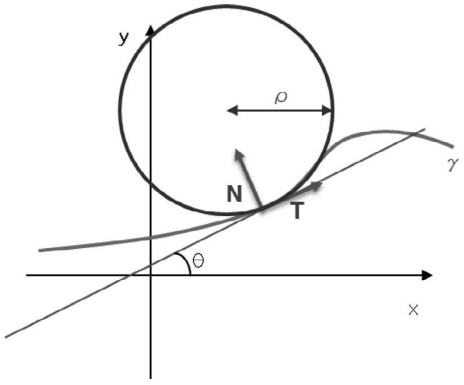

Fig. 1. Definition of tangential angle.

$$\frac{1}{\rho}=\frac{d\theta}{dx}=\frac{d\theta}{vdt}=\frac{\omega}{v}=\frac{\Delta v}{bv}. \quad \text{..... (3)}$$

However, ω in Eq. (3) is not the rotation speed of the strip but the time derivative of tangential angle $d\theta/dt$ which is defined as an angle between the tangent vector and the x-axis[1,2] (**Fig. 1**); $d\theta/dt$ depends only on the shape of the strip, and not on its rotation.

Also, the first assumption was based on the idea that the rotated angle of the strip at the delivery side θ_2 is reduced to rotated angle at the entry side θ_1 divided by λ. From the definition of curvature (Eq. (3)), they explained that additional curvature is generated by the rotation of the strip scaled by λ^2 because dx_2 increases to λx_1, whereas $d\theta_2$ decreases to $d\theta_2/\lambda$.

The basis of the first assumption was established in the first study[4] of side-slipping which represented the time-varying location of points on the centerline (**Fig. 2**). If the strip is regarded as a rigid body, the location of a point on its centerline can be represented as a function of time. If the longitudinal direction of the strip is defined as the x-axis, and the transversal direction of the strip as the y-axis, the velocity of the point $v(t)$ at time t can be represented as

$$v(t)=y\cdot\omega(t)+v_1(t), \quad \text{..... (4)}$$

$$u(t)=-x\cdot\omega(t), \quad \text{..... (5)}$$

where v, u are velocity along the x, and y-axis respectively, v_1 is the average speed of the strip at the entry side, and ω is the rotation speed of the strip. Then, time-varying location of the point $(x_1(t), y_1(t))$ at the entry side can be represented as

$$x_1(t)=x_0+\int_0^t v_1 dt \quad \text{..... (6)}$$

$$\begin{aligned} y_1(t) &= y_0-\int_0^t \omega_1(t)x(t)dt \\ &= f_0(x_1-v_1t)-\left[x_1\int_0^t\omega_1(t)dt-\int_0^t\left(\int_0^t\omega_1(t)dt\right)v_1dt\right]. \end{aligned} \quad \text{..... (7)}$$

Side-slipping is defined as the distance between centerline of the strip and center of the roll (x=0). Consequently, the model of side-slipping can be obtained as

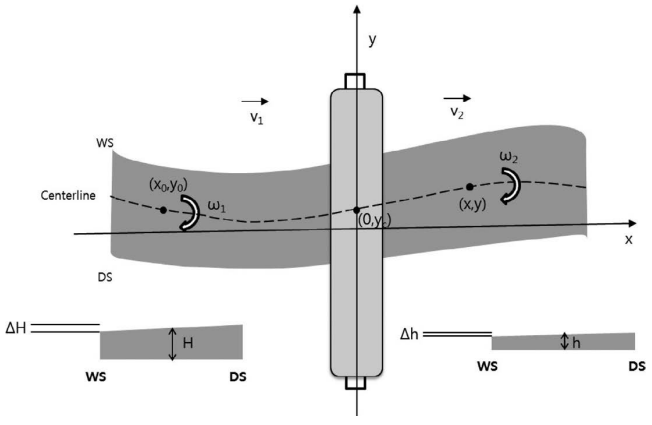

Fig. 2. Coordinate system of hot rolling process and cross-section of the strip.

$$y_c = f_0(-v_1 t) + v_1 \int_0^t \int_0^t \omega_1(t) dt dt. \quad \text{..... (8)}$$

Similar to Eqs. (6) and (7), the location of the point ($x_2(t)$, $y_2(t)$) at the delivery side can be represented as

$$x_2 = v_2(t-\tau) \quad \text{..... (9)}$$

$$y_2 = y_c(\tau) - v_2 \int_\tau^t \omega_2(t)(t-\tau) dt, \quad \text{..... (10)}$$

where τ is the time at which the point passes the center of the roll.

From Eqs. (4)–(7), tangential angle and curvature at the entry and delivery side can be represented as

$$\theta_1 = \frac{dy_1}{dx_1} = \frac{df_0(x_1 - v_1 t)}{dx_1} - \int_0^t \omega_1(t) dt \quad \text{..... (11)}$$

$$\frac{1}{\rho_1} = \frac{d^2 y}{dx_1^2} = \frac{d^2 f_0(x_1 - v_1 t)}{dx_1^2} - \int_0^t \omega_1(t) dt \quad \text{..... (12)}$$

$$\theta_2 = \frac{dy_2}{dx_2} = \left\{ -v_1 \frac{df_0(z)}{dz} + v_1 \int_0^\tau \omega_1(t) dt + v_2 \int_\tau^t \omega_2(t) dt \right\} \left(-\frac{1}{v_2} \right) \quad \text{..... (13)}$$

$$\frac{1}{\rho_2} = \frac{d^2 y}{dx_2^2} = \frac{d}{d\tau}\left(\frac{dy_2}{dx_2}\right)\frac{d\tau}{dx} = \frac{v_1^2}{v_2^2}\frac{d^2 f_0(z)}{dz^2} + \frac{v_1}{v_2^2} - \frac{1}{v_2}\omega_2(\tau). \quad \text{..... (14)}$$

Then the relations of tangential angle and curvature between entry and delivery side are

$$\theta_2 = \frac{\theta_1}{\lambda} \quad \text{..... (15)}$$

and

$$\frac{1}{\rho_2} = \frac{1}{\lambda^2}\left(\frac{1}{\rho_1} + \frac{\omega_1}{v_1}\right) - \frac{\omega_2}{v_2}. \quad \text{..... (16)}$$

In Eq. (13), θ_2 consists of three terms; the first one $-v_1 \frac{df_0(z)}{dz}$ is related to the original shape of the strip, the second one $-v_1 \int_0^\tau \omega_1(t) dt$ is the effect of rotation of the strip at the entry side, and the last one $-v_2 \int_\tau^t \omega_2(t) dt$ is the effect of rotation of the strip at the delivery side. That means the curvature change due to elongation difference was not considered but the effect of rotation of the strip is considered in the equation. From the definition of tangential angle dy/dx, Eq. (15) is natural because dx_2 increases to λdx_1 while dy_2 is remains the same.

To summarize, the previous model of curvature after rolling is based on two important assumptions. However, one of these assumptions is not true (Eq. (1)) because $1/\rho_1$ is not related to ω. Also, the basis of the effect $1/\rho_1$ on $1/\rho_2$ (Eq. (15)) is valid only when no elongation difference occurs at the delivery-side.

The inconsistency of Eq. (1) can be represented when a series of rolling stands are assumed (**Fig. 3**); $1/\rho_2$ is the delivery-side curvature at the first rolling stand (Fig. 3(a)), and also the entry-side curvature at the second rolling stand (Fig. 3(b)). $1/\rho_2$ can be represented using both $1/\rho_1$ and Δv_2 because it is delivery-side curvature at the first rolling stand (Fig. 3(b)), whereas it is also the entry-side curvature at the second rolling pass, and represented as only Δv_2 at the third rolling stand (Fig. 3(a)). Although these two curvatures should be identical, different definition were used in the existing model. To produce a reasonable explanation, curvature of the centerline should depend only on the velocity difference, and the effect of the entry-side curvature should be included in the delivery-side velocity difference.

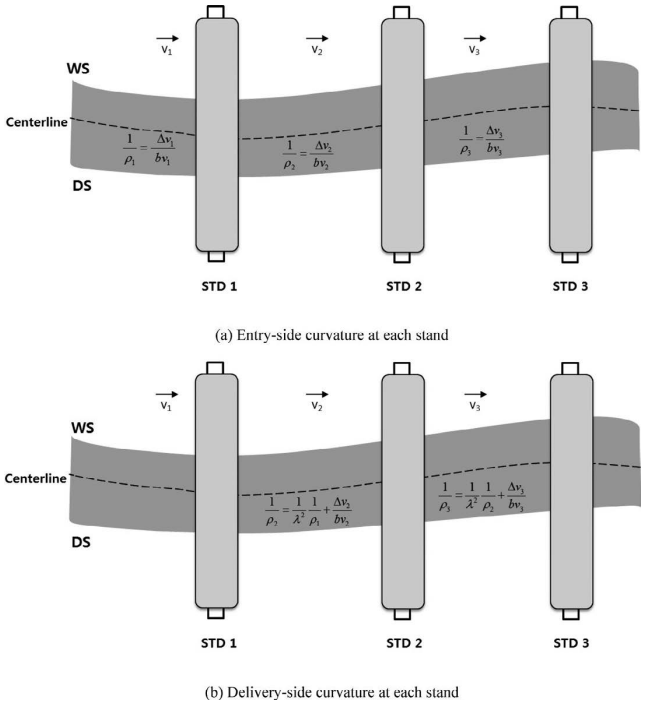

Fig. 3. Curvature of the bar at the multiple stands.

3. Proposed Delivery-Side Curvature Model

It is known that if the width of the bar is more than 10 times of thickness of it, strain in the width direction is under 3% which is not taken to be significant.[6] If the width of the strip b is assumed to not change during rolling, the thickness and velocity difference between DS and WS can be represented as

$$\begin{aligned} \Delta H &= (H_{DS} - H_{WS}) \\ \Delta v_1 &= (v_{1DS} - v_{1WS}) \\ \Delta h &= (h_{DS} - h_{WS}) \\ \Delta v_2 &= (v_{2DS} - v_{2WS}) \end{aligned}, \quad \text{..... (17)}$$

If the average value of thickness and velocity at the entry and delivery side are represented as

$$\begin{aligned} H &= \frac{H_{DS} + H_{WS}}{2} \\ v_1 &= \frac{v_{1DS} + v_{1WS}}{2} \\ h &= \frac{h_{DS} + h_{WS}}{2} \\ v_2 &= \frac{v_{2DS} + v_{2WS}}{2} \end{aligned}, \quad \text{..... (18)}$$

then the thickness and velocity of each side are obtained using Eqs. (17) and (18) as

$$\begin{aligned} H_{DS} &= H + \frac{\Delta H}{2} & H_{WS} &= H - \frac{\Delta H}{2} \\ v_{1DS} &= v_1 + \frac{\Delta v_1}{2} & v_{1WS} &= v_1 - \frac{\Delta v_1}{2} \\ h_{DS} &= h + \frac{\Delta h}{2} & h_{WS} &= h - \frac{\Delta h}{2} \\ v_{2DS} &= v_2 + \frac{\Delta v_2}{2} & v_{2WS} &= v_2 - \frac{\Delta v_2}{2} \end{aligned} \quad \text{..... (19)}$$

If the mass-flow principle is valid both in the DS (20) and the WS (21),

$$\left(H + \frac{\Delta H}{2}\right)\cdot\left(v_1 + \frac{\Delta v_1}{2}\right) = \left(h + \frac{\Delta h}{2}\right)\cdot\left(v_2 + \frac{\Delta v_2}{2}\right) \text{ .. (20)}$$

$$\left(H - \frac{\Delta H}{2}\right)\cdot\left(v_1 - \frac{\Delta v_1}{2}\right) = \left(h - \frac{\Delta h}{2}\right)\cdot\left(v_2 - \frac{\Delta v_2}{2}\right), \text{ .. (21)}$$

then substitution of (21) into (20) yields

$$H\cdot\Delta v_1 + \Delta H\cdot v_1 = h\cdot\Delta v_2 + \Delta h\cdot v_2. \text{ ..... (22)}$$

Due to the mass-flow principle $Hv_1 = hv_2$, so dividing the left side of Eq. (22) by Hv_1 and the right side by hv_2 yields

$$\frac{\Delta v_2}{v_2} = \frac{\Delta v_1}{v_1} - \left(\frac{\Delta h}{h} - \frac{\Delta H}{H}\right) = \frac{\Delta v_1}{v_1} - \Delta\psi. \text{ ..... (23)}$$

To formulate the $1/\rho_2$ as an equation that includes Δv_2, the definition of curvature and tangential angle are used. At the entry side of rolling (**Fig. 4**(a)), entry-side velocity at the centerline of the strip v_1 is constant, then the length ds_1 that the strip moves into the roll during infinitesimal time dt is constant. When a cambered strip is fed into the roll for constant distant ds_1, the length of the strip which is fed into the roll is different at the work side and drive side.

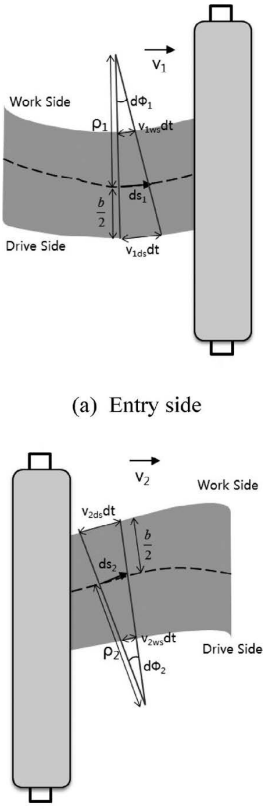

(a) Entry side

(b) Delivery side

Fig. 4. Relation between curvature and velocity difference.

From Eq. (8), ds_1 can be represented as curvature multiplied by differential tangential angle. Because ρ_1 is the radius of the circle that approximates the arc that ds_1 makes (Fig, 4(a)), the differential of tangential angle $d\theta_1$ is equal to the differential of subtended angle $d\phi_1$:

$$ds_1 = v_1 dt = \rho_1 d\theta_1 = \rho_1 d\phi_1 \rightarrow \frac{v_1}{\rho_1} = \frac{d\phi_1}{dt}. \text{ ..... (24)}$$

When the centerline of the strip is fed distance ds_1 into the roll, the lengths that strip at the drive side and work side feeds into the roll are

$$\begin{aligned} ds_{1,ds} &= v_{1ds} dt = d\phi_1\left(\rho_1 + \frac{b}{2}\right) \\ ds_{1,ws} &= v_{1ws} dt = d\phi_1\left(\rho_1 - \frac{b}{2}\right) \end{aligned}. \text{ ..... (25)}$$

Therefore, velocity difference can be represented as the equation that includes $d\phi_1$ as

$$v_{1ds}dt - v_{1ws}dt = \Delta v_1 dt = b d\phi_1 \rightarrow \Delta v_1 = b\frac{d\phi_1}{dt}. \text{ .... (26)}$$

From Eqs. (24) and (26), the relation between Δv_1 and $1/\rho_1$ is obtained as

$$\frac{\Delta v_1}{b v_1} = \frac{1}{\rho_1} \text{ ..... (27)}$$

$$\frac{\Delta v_2}{b v_2} = \frac{1}{\rho_2}. \text{ ..... (28)}$$

Similar analysis can be applied to the delivery side as (Fig. 4(b)) to yield Eq. (28). Using Eq. (23) we obtain a model for $1/\rho_2$ curvature at the delivery side as

$$\frac{1}{\rho_2} = \frac{1}{v_2}\frac{d\phi_2}{dt} = \frac{\Delta v_2}{b\cdot v_2} = \frac{1}{b}\cdot\left(\frac{\Delta v_1}{v_1} - \Delta\psi\right) = \frac{1}{\rho_1} - \frac{\Delta\psi}{b}. \text{ ..... (29)}$$

Compared to Eq. (29), Eq. (1) has scaling terms related to the λ, and different signs for the $\Delta\psi$. The previous studies assumed that $1/\rho_2$ of the strip will be influenced by $1/\rho_1$ scaled by the λ^2 due to the rotation of the strip at the entry side ω_1. Also they showed that Δv_2 is proportional to the $\Delta\psi$. As a result, $1/\rho_2$ is not only affected by the Δv_2 but also by $1/\rho_1$. In contrast, the proposed delivery-side curvature model is constructed based on the fact that elongation difference is the cause of a curved strip. Δv_2 is represented as Δv_1 and $\Delta\psi$ (Eq. (23)). Because Δv_1 is related to $1/\rho_1$ and is already included in Δv_2, the inconsistency that was shown in Section 2 is not generated.

4. Results

4.1. Set-up

The FEM is used to build a simulator for the hot rolling process to verify the accuracy of the proposed model of delivery-side curvature. To simplify the process and to reduce simulation time, the FEM simulator was composed only of roll, strip, and pusher using mirror symmetry on the lower side of the bar (**Fig. 5**) with the aid of the commercial

FEM software DEFROM 3D. The roll was assumed to be a rigid body, and the strip was assumed to be a rigid plastic body. Consequently, the thickness of the strip was equal to the roll gap. The bar was assumed as AISI 1015 carbon steel, and yield strength of the material was 325 MPa. Shear friction coefficient was set as 0.7.[7] More detailed specifications of the simulator are shown in **Table 1**.

The simulator implemented 130 steps of simulation: each simulation step describes 0.05 s of the rolling process and was composed of rolling and tilting processes. During the rolling process, the strip was rolled for 0.05 s with a roll gap difference which was adjusted during the tilting process.

The DEFORM 3D cannot design a curved strip directly.

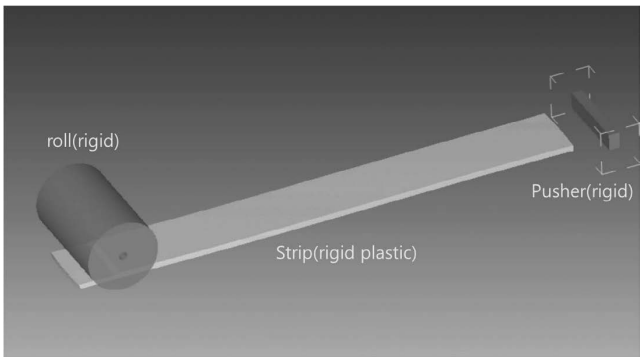

Fig. 5. FEM simulator configuration.

Table 1. Dimensions of simulator.

Quantity	Value
Entry-side thickness	105 (mm)
Delivery-side thickness	85 (mm)
Entry-side velocity	1 500 (mm/s)
Delivery-side velocity	1 853 (mm/s)
Length before rolling	9 166 (mm)
Length after rolling	11 113 (mm)
Width of the strip	1 200 (mm)
Radius of roll	650 (mm)
Width of roll	2 080 (mm)
Shear friction	0.7
Temperature of the strip	1 200°C
Temperature of the roll	20°C

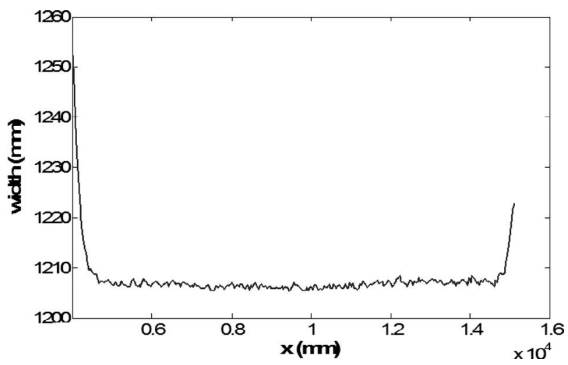

Fig. 6. Width variation after rolling.

For this reason, a strip that had a straight rectangular shape was designed and rolled with a predefined history of roll gap difference to produce a curved strip that had a wedge. Two test bars were produced in this way: Test Bar 1 (**Fig. 7**(a)) had an 'S' shape and 2.5-mm maximum entry-side wedge (**Fig. 8**(a)). Test Bar 2 (Fig. 7(b)) had a 'C' shape and maximum 3.5-mm entry-side wedge deviation (Fig. 8(b)).

The two test bars were composed of hexahedral elements: 301 layers of cross sections composed of 138 nodes. Among them, 301 nodes in the mid-width of the upper side were regarded as the centerline of the strip and were used when calculating its curvature. Locations of the nodes that consist centerline of the strip was extracted from the simulator, and fitted to a 10th order polynomial using least squares regression. The curvature of the centerline was calculated from this polynomial.

4.2. Results

Because the new model is obtained using the assumption that width of the bar is not changed during rolling, we first verified width variation after rolling. In simulation, there was no restriction in width variation of the bar. The results show that width variation is ignorable except head and tail part of the bar (**Fig. 6**). Width of the bar is increased about 7 mm and the value is less than 0.6% of the bar width. Width of the bar at the head and tail part increased up to 50 mm and 20 mm, nevertheless, these parts are extremely small than other parts.

The accuracy of the new model of curvature (Eq. (29)) at the delivery side was verified using FEM simulation and compared to the old model (Eq. (1), with ξ as 1) for two

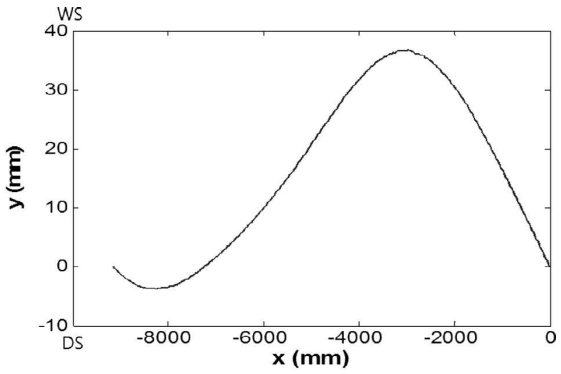

(a) Test Bar 1

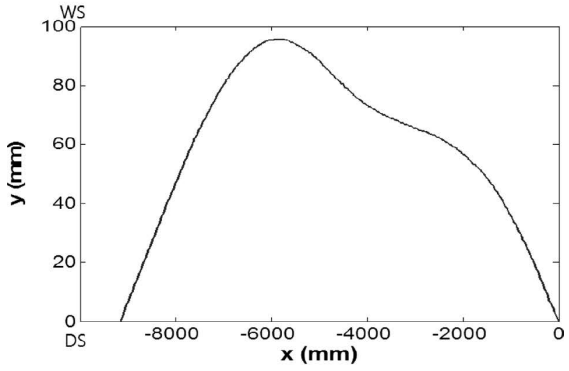

(b) **Test Bar 2**

Fig. 7. Centerline of the two Test Bars before rolling.

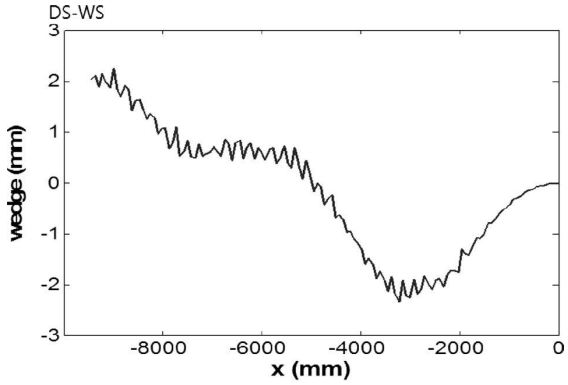

(a) **Test Bar 1**

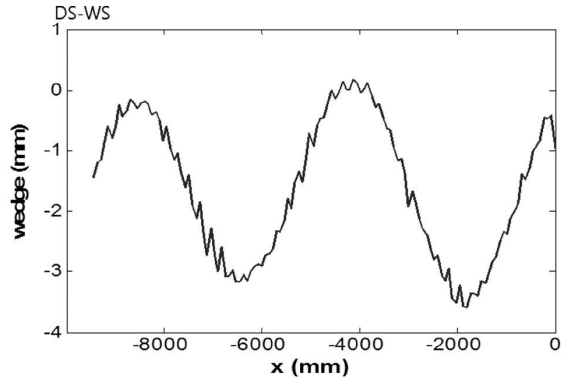

(b) **Test Bar 2**

Fig. 8. Entry-side wedge of the two Test Bars.

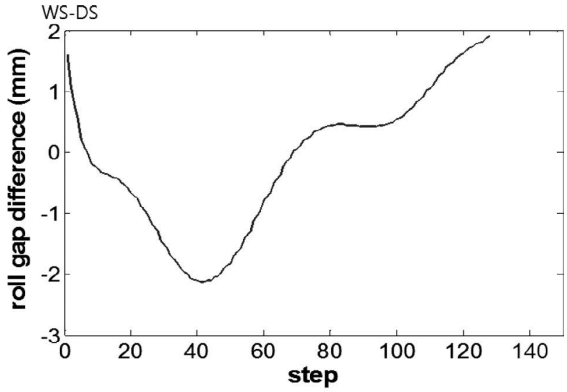

(a) Test Bar 1

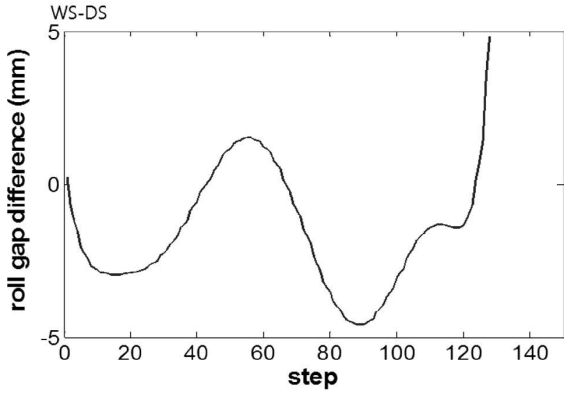

(b) Test Bar 2

Fig. 9. History of roll gap difference.

test bars. Two test bars were rolled with histories of roll gap difference (**Fig. 9**). As a result, strips having reasonable amount of curvature were generated. Predicted curvatures were calculated from the proposed model (Eq. (29)) and the old model (Eq. (1)) using measured wedge (Fig. 8), entry-side curvature (**Fig. 10**), and delivery-side wedge (**Fig. 11**). Measured and predicted curvatures were compared (**Fig. 12**).

For the Test bar 1 (Fig, 12(a)), the old model predicted delivery-side curvature well when it was between $\pm 5 \times 10^{-6}\,(\mathrm{mm}^{-1})$, but beyond this range, error increased up to $10^{-5}\,(\mathrm{mm}^{-1})$. In contrast, the value predicted by using Eq. (29) was within $5\times10^{-6}\,(\mathrm{mm}^{-1})$ of the measured value. For the Test bar 2 (Fig. 12(b)), the curvatures predicted by the old model had significant error at two peak points whereas those from the new model are very close to the measured values.

Even though the old model and the new model differ only by the scaling factor λ, the new model predicts the curvature better than does the old model. Especially when the measured curvature is large, the old model predicts much less curvature than does the new model. This means that the old model underestimates the curvature of the strip. These simulation results indicate that the proposed model is more precise than the old model.

Calculated curvatures oscillate due to the entry-side wedge (Fig. 8). The wedge of the strip was measured by subtracting the thickness of the drive-side from the work-side in the same layer. As a result, measurement error was generated when the strip did not go straight to the roll.

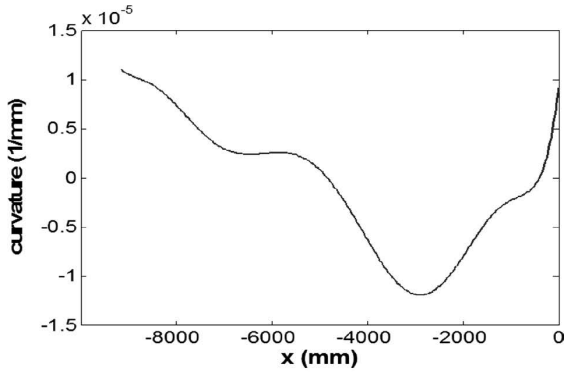

(a) Test Bar 1

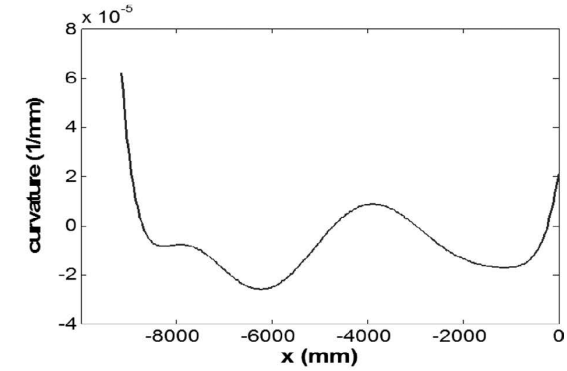

(b) Test Bar 2

Fig. 10. Curvature of the two Test Bars before rolling.

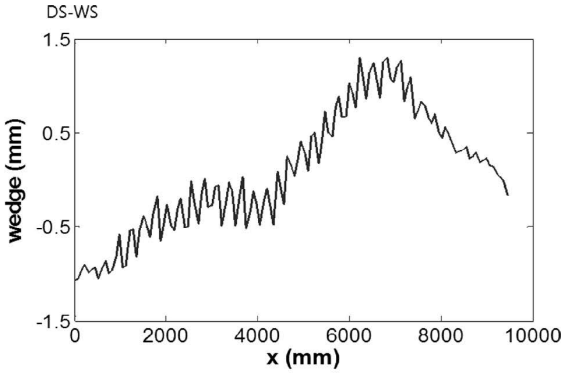

(a) Test Bar 1

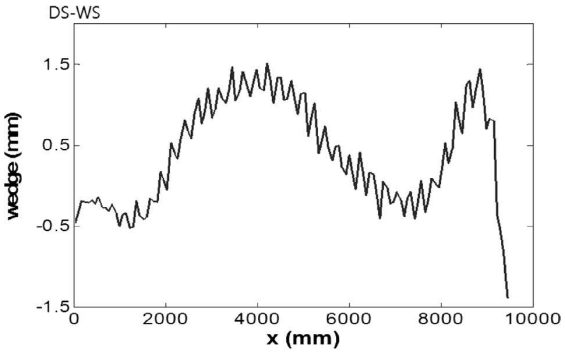

(b) Test Bar 2

Fig. 11. Delivery-side wedge of the two Test Bars.

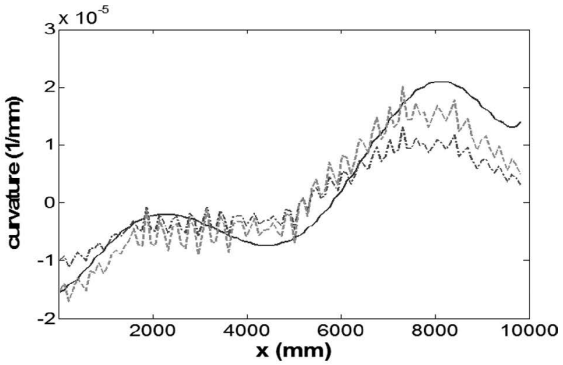

(a) Test Bar 1

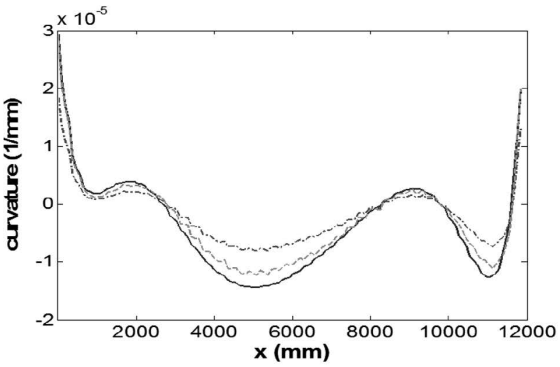

(b) Test Bar 2

Fig. 12. Curvature calculated by old (Eq. (1), green dash-dot line) and new (Eq. (29), red dash line) model; blue line: measured curvature at the delivery side.

5. Conclusion

This paper presents a new model that describes the change in curvature of strip at the delivery side during hot rolling process. An inconsistency of the existing model is pointed out. Based on the definition of the curvature, tangent vector, and tangential angle, the velocity difference between DS and WS of the strip is represented as the curvature of the centerline. Assuming that the mass-flow principle is valid both in DS and WS, the velocity difference at the delivery side is represented as the sum of entry-side velocity difference and wedge ratio. A new mathematical model for curvature of the centerline is represented as an equation that includes entry-side curvature and wedge ratio. To evaluate the accuracy of the proposed model, an FEM simulator for the hot rolling process was developed. The simulation results show that proposed model is more accurate than the existing model.

REFERENCES

1) J. W. Rutter: Geometry of Curves, Chapman & Hall/CRC, London, (2000), 1.
2) A. Pressley: Elementary Differential Geometry, Springer-Verlag, London, (2001), 1.
3) Y. Tanaka, K. Omori, T. Miyake, K. Nishizaki, M. Inoue and S. Tezuka: *Kawasaki Steel Giho*, **16** (1987), 12.
4) K. Nakajima, T. Kajiwara, T. Kikuma, T. Kimura, H. Matsumoto, M. Tagawa, Y. Shirai and K. Yoshimoto: Proc. 1981 Japanese Spring Conf. for the Technology of Plasticity, JSTP, Tokyo, (1981), 147 (in Japanese).
5) T. Shiraishi, H. Ibata, A. Mizuta, S. Nomura, E. Yoneda and K. Hirata: *ISIJ Int.*, **31** (1991), 583.
6) J. Lenard: Primer on Flat Roling, Elsevier, London, (2007), 1.
7) E. Ceretti, C. Giardini and L. Giorleo: *Int. J. Mater. Form.*, **3** (2010), 323.